Display of Pixel Loss and Replication in Reprojecting Raster Data from The Sinusoidal Projection

Denis White
US Environmental Protection Agency
200 SW 35th Street
Corvallis, Oregon 97333 USA
E-mail: white.denis@epa.gov

Abstract

Recent studies show the sinusoidal projection to be a superior planar projection for representing global raster datasets. This study uses the sinusoidal projection as a basis for evaluating pixel loss and replication in eight other planar map projections. The percent of pixels represented accurately as a single pixel when projected from the sinusoidal to one of the other projections ranged from a low of about 58% for the Van der Grinten projection to a high of about 83% for the Mollweide projection. The graphic display of these losses and gains of pixels had revealing patterns, for example, large values of replication in the higher latitudes of cylindrical projections.

Introduction

Recent articles have analyzed and illustrated resampling errors in the form of pixels lost and replicated when raster datasets are projected between the sphere and the plane using various map projections. These errors are potentially an important effect in many applications. For example, in using categorical data such as classified imagery displayed over large areas like continents, hemispheres, or the entire globe, the distribution of pixel counts by class can change substantially depending upon the projection. Similarly, the distributions of continuous data can change as well.

Steinwand *et al*. (1995) initiated the recent series of articles by describing the nature of the problem and then analyzing and displaying the distortion produced for several combinations of projections using alternating black and white checkerboard image blocks. Mulcahy (2000) developed measurements for pixel loss and duplication and analyzed these properties for eight projections. Mulcahy and Clark (2001) reviewed the display of map projection distortions in general, including the techniques developed by Steinwand *et al*. (1995) for raster data distortions.

Kimerling (2002) developed another approach to measuring and displaying pixel loss and replication called the data loss and duplication map and applied this to projections of equal angle raster data (grids with equal increments in latitude and longitude). Seong and Usery (2001) and Seong (2003) developed a scale factor model of the accuracy of the transfer of categorical raster data and applied the model to transfers between each pairwise combination of three different projections. Seong *et al*. (2002) calculated the accuracy of the transfer of generic categorical raster data between UTM and five other projections. Usery and Seong (2001) and Usery *et al*. (2003) calculated the accuracy of the transfer of specific categories of several databases between pairwise combinations of a number of projections.

One notable finding in Mulcahy (2000), Seong and Usery (2001), and Seong *et al*. (2002) was the evidence for the superior performance of the sinusoidal projection in minimizing raster data resampling errors. The Seong papers (2001, 2002) explained the mathematical basis for the sinusoidal projection's performance as a result of the projection's horizontal scale factor being equal to 1.0 along all parallels of latitude. This property means that, for example, equally spaced horizontal transects in the projection space have equally spaced transects on the sphere. Furthermore, parallels are equally spaced vertically. Thus square pixels in the projection space sample equal increments in both longitude and latitude on the sphere, whereas other projections do not have this property. It is worth noting that the sinusoidal projection would not necessarily have this advantage for some alternative planar tessellation systems, such as hexagons.

Because the vast majority of rasterized data uses square grids, however, it is useful to have techniques to assist in evaluating the effects of projection distortion on pixel loss and replication. Using the sinusoidal projection as a basis and square pixels, this paper presents the pixel loss and replication patterns for eight other projections.

Methods

Loss and replication patterns of eight projections were

Table 1 Percent of pixels lost, matched, or replicated (gained), plus the maximum number of replicated pixels, all relative to the Sinusoidal projection. Classes of replicated pixels are the same as those of Figure 2.

Projection	Loss	1-1	Gain 2-4	Gain 5-8	Gain 9+	Max Gain
Sinusoidal	0.0	100.0	0.0	0.0	0.0	1
Van der Grinten	0.0	57.8	28.8	9.8	4.1	500
Miller	0.0	63.4	23.7	9.6	4.0	321
Robinson	13.3	76.3	9.8	0.5	0.1	89
Plate Carrée	0.0	68.8	27.3	3.4	0.9	401
Mollweide	8.7	82.8	8.6	0.0	0.0	5
Hammer-Aitoff	10.0	80.1	10.0	0.0	0.0	2
Eckert IV	15.1	71.0	13.7	0.2	0.0	6
Gall-Peters	21.9	58.2	19.5	0.3	0.0	27

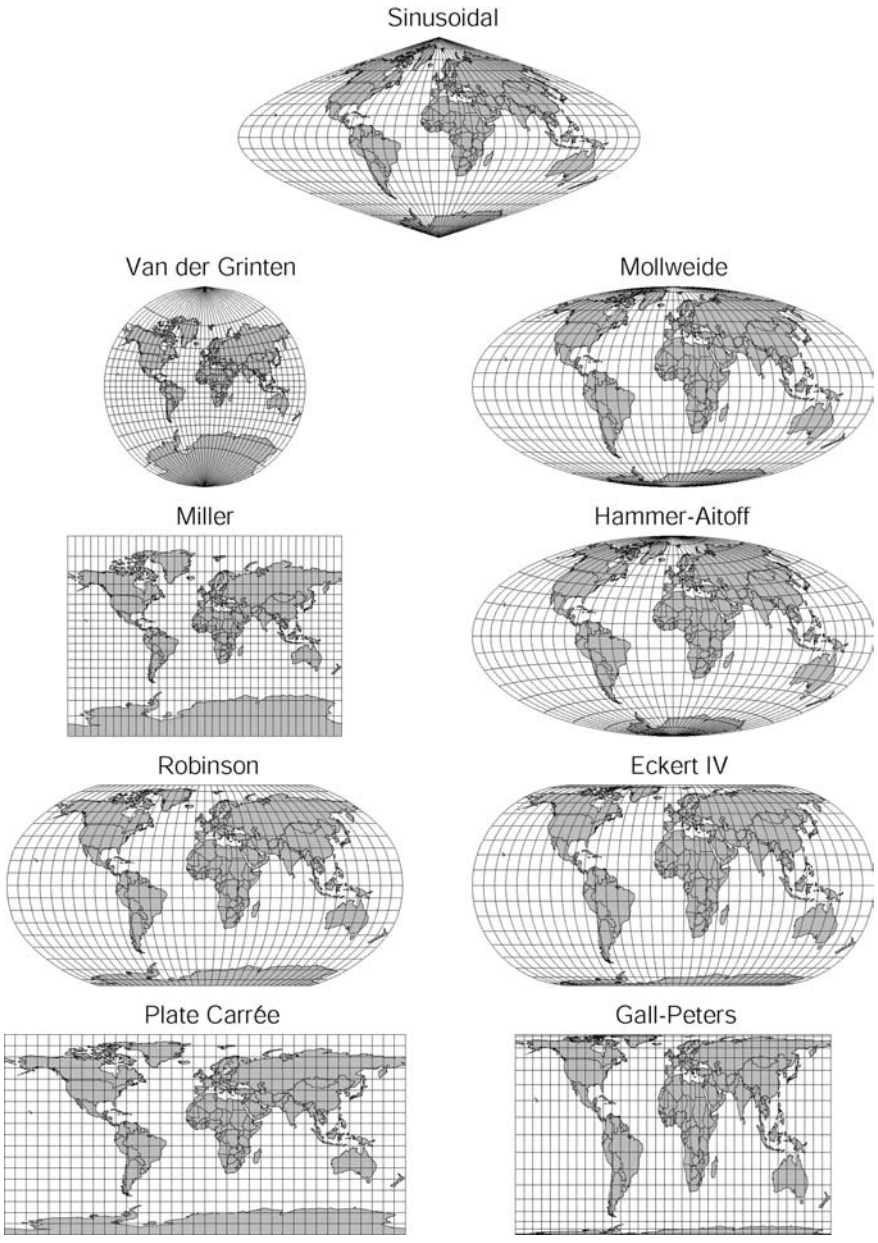

Figure 1 Longitude and latitude graticules and continental land masses shown in map projections used in the analysis.

examined, four equal area projections and four that were not equal area. The four non-equal area projections were the Van der Grinten, Miller, Robinson, and Plate Carrée. The equal area projections were the Mollweide, Hammer-Aitoff, Eckert IV, and Gall-Peters. The last is given its name here in recognition of its initial publication by James Gall, even though Arno Peters republished it with minor modification in the late 20th Century (and both Gall's and Peters' versions being modifications of Lambert's equal area cylindrical projection).

Each projection was sampled in its planar projection space with a tessellation of squares of 100 kilometers on a cell side. The coordinates of the grid samples were projected to geographic space (latitude and longitude coordinates) and then reprojected to the sinusoidal projection, rounding to the nearest sinusoidal grid position. Both forward and inverse projections were performed using spherical rather than ellipsoidal models of the earth; formulae were obtained from Snyder (1990, for the Robinson projection), Maling (1974, for the Hammer-Aitoff forward projection), Wolfram Research (1999-2005, for the Hammer-Aitoff inverse projection), and Snyder (1987, for all others). The number of samples of the given projection that occurred in each 100 km cell of the sinusoidal projection space was recorded. The sample counts, for each projection, in each

pixel of the sinusoidal space were mapped in the sinusoidal space, using the classes of 0 (pixels that were lost), 1 (pixels in the original projection that became exactly one pixel in the sinusoidal), gain (pixels that were replicated in the sinusoidal) of 2-4 pixels, gain of 5-8 pixels, and gain of 9 or more pixels. The maximum number of replicated pixels for each projection in any pixel of the sinusoidal projection was also recorded.

Results and discussion

The number of pixels of the different projections for each cell in the sinusoidal projection ranged from 0 (pixels lost) to a maximum of 500 (a replication of 500 Van der Grinten pixels in one sinusoidal pixel) (Table 1).

Mapped patterns of loss and replication highlight aspects of the behavior of the different projections (Figure 2). The non-equal area projections displayed substantially more pixel replication, especially in high latitudes, which is not surprising. The Robinson projection was an exception to this pattern. The equal area projections displayed a balancing between losses and gains necessary to achieve equal area representation. The graphic patterns show the effects of aliasing caused by the square wave transfer function from the nearest neighbor resampling (Russ 1995, also see, for examples, http://geospatialmethods.org/smmrpfreport/, accessed 5 November 2004). All eight projections had symmetric patterns across the equator and across the central meridian. The Hammer-Aitoff projection had a distorted four-way symmetry that might be expected from a stretched azimuthal projection.

The bar charts of losses and gains (Figure 3) show more dramatically some aspects of the statistics of Table 1 and they summarize the patterns in Figure 2. The size of the bars in each projection's graph is an indication of how many levels of replication the projection had. The Van der Grinten projection, for example, had the greatest variety in replication, and the Hammer-Aitoff the least, having only duplicates. The non-equal area projections, except for the Robinson projection, had no losses of pixels.

The idea of a data loss and duplication map was introduced by Kimerling (2002) to display the spatial pattern of resampling error due to map projections. In that paper the maps were applied to projections from equal angle data sets to planar surfaces. This paper draws on the work of Seong and collaborators which shows the superiority of the sinusoidal projection in representing raster data. In recognition of this superiority, several global datasets are now being distributed in this projection, for example, the Integerized Sinusoidal (ISIN) MODIS land products (http://lpdaac.usgs.gov/landdaac/tools/modis/index.asp, accessed 5 November 2004), and the Mars Mosaicked Digital Image Model (MDIM) (http://pdsimage2.wr.usgs.gov/cdroms/viking_orbiter/vo_2007/document/volinfo.txt, accessed 5 November 2004).

If the sinusoidal projection becomes more commonly used for distributing global datasets, as is appropriate, then it will become more important to better understand the nature of resampling errors from that projection. To this end,

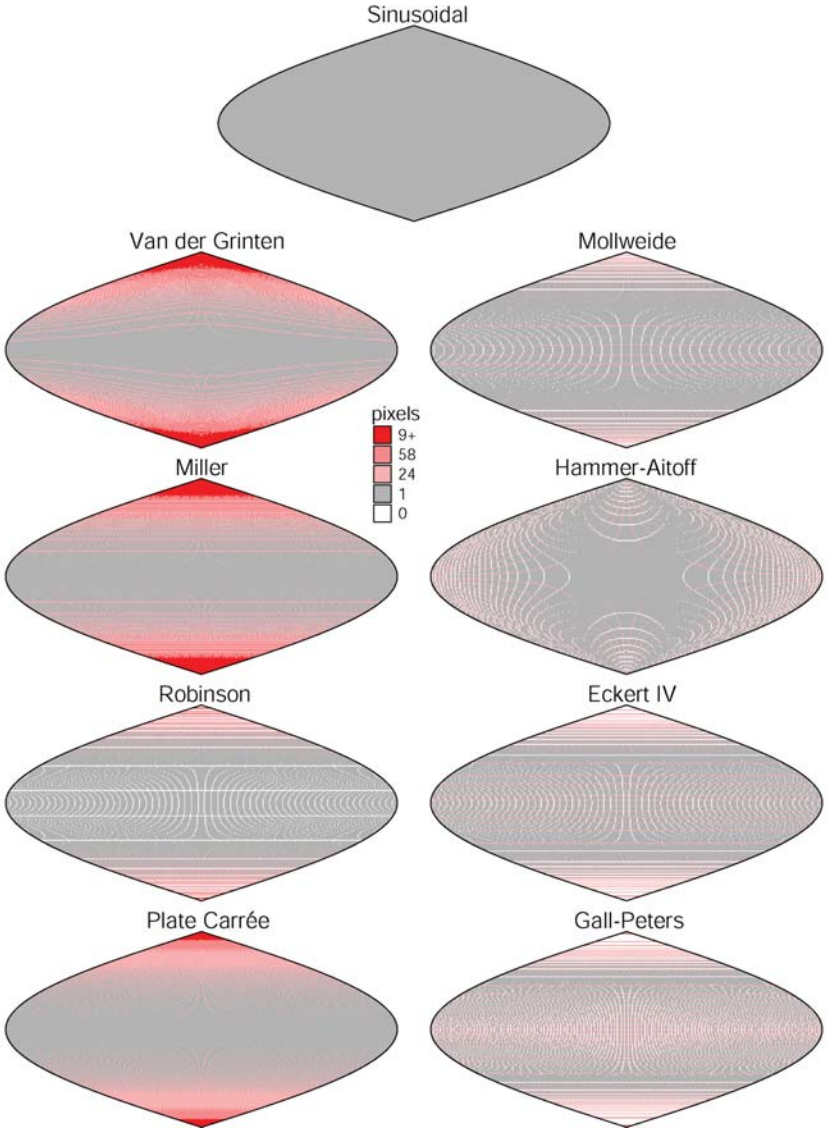

Figure 2 Maps of pixel loss and replication for each projection relative to the sinusoidal projection, which was used as the base map. All maps (except the sinusoidal) show graphic patterns similar to Moiré patterns, where the nearest neighbor resampling to the sinusoidal projection produced intersecting patterns of curved or straight, white or pink, lines on a gray background.

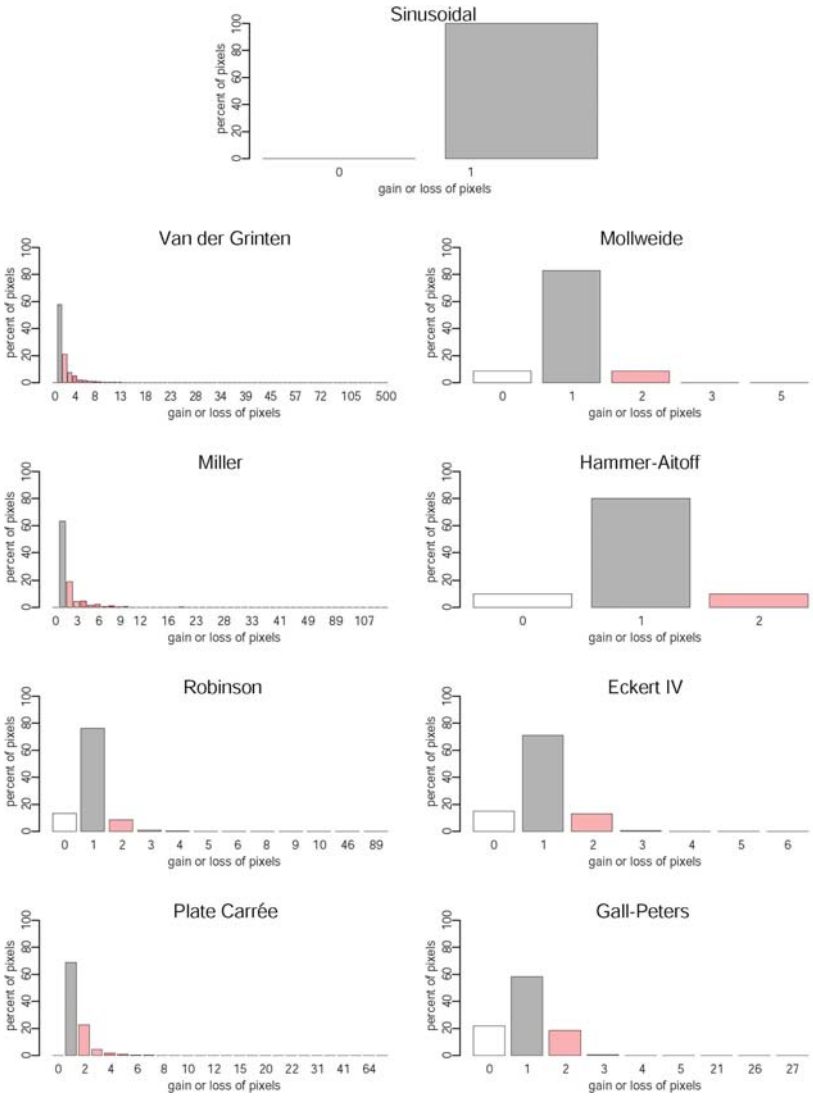

the maps and graphs presented in this paper present a graphical method to portray that understanding.

R language programs for these analyses are available from the author.

Acknowledgements.

Jon Kimerling and Jeong Chang Seong have kindly reviewed an initial version of this manuscript and helpful comments were provided by the journal editor. The research described in this article has been funded in part by the US Environmental Protection Agency. The manuscript has been subjected to the Agency's peer and administrative review and approved for publication. Approval does not signify that the contents reflect the views of the Agency, nor does mention of trade names or commercial products constitute endorsement or recommendation for use.

References

Kimerling, A. J., 2002. Predicting data loss and duplication when resampling from equal-angle grids. *Cartography and Geographic Information Science*, 29:111-126.

Maling, D. H., 1973. Coordinate Systems and Map Projections. George Philip and Son Limited, London, UK. 255 p.

Mulcahy, K. A., 2000. Two new metrics for evaluating pixel-based change in data sets of global extent due to projection transformation. *Cartographica*, 37:1-11.

Mulcahy, K. A. and K. C. Clarke, 2001. Symbolization of map projection distortion: a review. *Cartography and Geographic Information Science*, 28:167-181.

Russ, J. C., 1995. *The Image Processing Handbook, 2nd Edition*. CRC Press, Boca Raton, FL. 674 p.

Seong, J. C., 2003. Modelling the accuracy of image data reprojection. *International Journal of Remote Sensing*, 24:2309-2321.

Seong, J. C. and E. L. Usery, 2001. Assessing raster representation accuracy using a scale factor model. *Photogrammetric Engineering & Remote Sensing*, 67:1185-1191.

Seong, J. C., K. A. Mulcahy, and E. L. Usery, 2002. The sinusoidal projection: a new importance in relation to global image data. *The Professional Geographer*, 54:218-225.

Snyder, J. P., 1987. Map Projections—A Working Manual. U.S. Geological Survey Professional Paper 1395. United States Government Printing Office, Washington, DC. 383 p.

Snyder, J. P., 1990. The Robinson projection—a computation algorithm. *Cartography and Geographic Information Systems*, 17:301-305.

Steinwand, D. R., J. A. Hutchinson, and J. P. Snyder, 1995. Map projections for global and continental data sets and an analysis of pixel distortion caused by reprojection. *Photogrammetric Engineering & Remote Sensing*, 61:1487-1497.

Usery, E. L. and J. C. Seong, 2001. All equal-area map projections are created equal, but some are more equal than others. *Cartography and Geographic Information Science*, 28:183-193.

Usery, E. L., M. P. Finn, J. D. Cox, T. Beard, S. Ruhl, and M. Bearden, 2003. Projecting global datasets to achieve equal areas. *Cartography and Geographic Information Science*, 30:69-79.

Wolfram Research, 1999-2005. Hammer-Aitoff Equal-Area Projection. URL: http://mathworld.wolfram.com/Hammer-AitoffEqual-AreaProjection.html, (accessed 30 August 2005).

Figure 3. Bar graphs of the losses and gains of pixels for each projection relative to the sinusoidal projection. Each bar shows the number of pixels for a single value of losses or gains. "0" is a pixel in the sinusoidal projection that was lost from the given projection; "1" is a pixel that was transferred without gain or loss; "2" is a pixel in the sinusoidal that was covered by two pixels in the given projection; and so forth. The Van der Grinten and Miller projections had more values of replication than can be shown in the labels at the bottom of the bars; only a sample of those values is indicated.